

Response of a Global Ocean Circulation Model to Real-Time Forcing and Implications to Earth's Rotation

J. SEGSCHNEIDER AND J. SÜNDERMANN

Institute of Oceanography, University of Hamburg, Hamburg, Germany

(Manuscript received 20 November 1995, in final form 3 March 1997)

ABSTRACT

The ocean's contribution to interannual variations in length of day (lod) is investigated by means of the global Hamburg large-scale ocean circulation model (LSG) forced with observed wind stress and air temperature fields. The horizontal resolution of the model is 3.5° in latitude and longitude, and eleven layers exist in the vertical; the timestep used is one month. The atmospheric forcing is obtained by adding ECMWF 1000-mb monthly anomalies of wind stress and air temperature to climatological values of Hellerman and Rosenstein and COADS, respectively. The data extend from November 1979 to November 1993. Within this period three El Niño events (1982–83, 1986–87, and 1991–92) and two La Niña events (1984, 1988) were observed. Variations in the pressure torque, the inertia tensor of the ocean, and the momentum connected with the currents are calculated diagnostically from the OGCM output. Model results show that the ocean works mainly as a transmitter of angular momentum from the atmosphere to the solid earth and that contributions to interannual variations of lod from the mass distribution term amount to four times the effect of the motion term. Contributions to interannual variability of lod can mainly be attributed to the pressure torque and the matter term, whereas the contribution by the ocean currents varies on shorter timescales up to one year. The calculated total changes in lod are in the order of 0.1 ms. This is the right order of magnitude to close the imbalance between observed changes and results from atmospheric circulation models, but the correlation between observed residuals and computed anomalies is still poor.

1. Introduction

It is well known (Munk and MacDonald 1960) that changes in the atmospheric circulation cause changes in the length of day (lod) and wobble (i.e., change of the orientation of the earth's rotation axis in space) on time-scales of days to months, while interannual variations can be attributed to the ocean's response to the atmospheric forcing.

Observations of lod have been made since about 1860 (Rosen and Salstein 1986). A part of the observed variability is thought to be explained by the atmosphere's and ocean's dynamics. As an example, time series of observed anomalies in lod and sea surface temperature of the equatorial Pacific show remarkably high correlation (Rosen et al. 1984; Salstein and Rosen 1984; Zheng et al. 1990). Here we focus our efforts on the oceanic contribution in the interannual time range based on the Hamburg Large Scale Ocean Model (LSG). The model is forced with wind stress and air temperature anomalies derived from ECMWF data over the period November 1979–November 1993.

The influence of the ocean on the rotation rate of the solid earth can be split up into three parts. First, like the mountain torque between atmosphere and solid earth, torques at the topographic boundaries are exerted due to zonal sea level and density gradients (Peixoto and Oort 1992). Second, the moment of inertia of the ocean is changed by vertical and meridional mass redistributions, that is, by changing the distance of the fluid elements to the rotation axis. Third, momentum is stored or released by zonal currents, primarily in the Antarctic Circumpolar Current (ACC). The atmosphere–solid earth–ocean system has an almost closed momentum budget. Thus, the difference between astronomical observations of lod (that means the rotation rate of the solid earth) and momentum stored in the atmosphere as computed by AGCMs should be explained by the ocean's contribution. Motions within the fluid core and the ice cover are assumed to be constant over periods of some ten years (Lambeck 1980). Furthermore, the contributions of the groundwater cycle (i.e., the distribution of freshwater in rivers, lakes, and ground) and the freshwater fluxes between ocean and atmosphere (i.e., precipitation minus evaporation) are not considered here, as well as the possible role of the earth's crust (Peixoto and Oort 1992) because their quantities are unknown.

The computed time series of the pressure torque, the

Corresponding author address: J. Segsneider, Max-Planck-Institut für Meteorologie, Bundesstrasse 55, D-20146 Hamburg, Germany.
E-mail: segsneider@dkrz.de

moment of inertia, and the momentum stored in ocean currents are analyzed. El Niño-related zonal sea level and density gradient changes in the equatorial Pacific are discussed as well as changes of the meridional mass distribution that result in changes of the moment of inertia. The LSG has been chosen to perform the experiment because the coarse resolution and the long time step of one month allow model integrations without relaxation to climatological hydrographic data (Levitus 1982) at any depth. The currently available high-resolution models are relaxed to Levitus climatological hydrographic data (e.g., at the surface and below 700 m in Ponte and Rosen 1994). As Levitus data are only resolving a mean seasonal cycle, this may result in an underestimation of interannual variation of the ocean.

The paper is structured as follows: In section 2 the model and the setup of the numerical experiment are described together with a comment on the forcing data. In section 3 the single terms of the momentum balance are explained and the model results are discussed. Conclusions are given in section 4.

2. Model description, forcing data, and setup of the numerical experiment

The experiment is started from an equilibrium state of the large-scale geostrophic ocean model, developed at the Max-Planck-Institut für Meteorologie in Hamburg (Maier-Reimer et al. 1993), after 4000 years of integration. The model is forced by climatological wind stress (Hellerman and Rosenstein 1983, hereafter HR), air temperatures from the Comprehensive Ocean Atmosphere Data Set (COADS; Woodruff et al. 1987) and freshwater fluxes derived from former runs with prescribed annual mean surface salinity (Levitus 1982). The seasonal cycle is resolved by a time step of one month, the horizontal resolution is 3.5° on an Arakawa E-grid; the topography is realistic within this limitation. The model has 11 layers with a finer resolution in the upper part of the water column. The centers of the layers are at 25 m, 75 m, 150 m, 250 m, 450 m, 700 m, 1000 m, 2000 m, 3000 m, 4000 m, and 5000 m. The model has a free-slip condition at the bottom, but lateral friction at the side walls. The hydrostatic and Boussinesq approximations are used.

The transient boundary conditions are 24-h forecasts (6 h from 1990 on) extending from November 1979 to November 1993. The data are computed at the European Centre for Medium-Range Weather Forecasts and processed by the "Deutscher Wetterdienst" in Köln. To construct a consistent dataset, we used midnight values (0000 UTC) throughout the whole period. The higher resolution from January 1990 on allowed us to check whether the 0000 UTC choice causes some bias toward day/night area spatial patterns. It turned out that the effect was small for the wind stress and air temperature in oceanic regions.

To force the OGCM, a hybrid dataset is constructed.

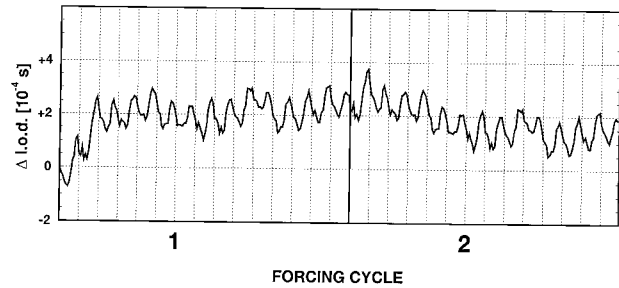


FIG. 1. Time series of Δlod attributed to the matter term for the two forcing periods. Forcing period one extends from 1979 to 1993 and forcing period two from 1980 to 1993, as for 1979 ECMWF data are available only for November and December. The horizontal unit is years.

It consists of HR and COADS climatological values and ECMWF anomalies (Segsneider 1991; Winguth et al. 1994). Anomalies are obtained by calculating wind stress from the midnight daily ECMWF 1000-mb vorticity and divergence fields and then averaging this stress monthly in a first step. In a second step the January mean, the February mean, and so on for the whole period are calculated (representing the mean climatological values of the dataset), and in a third step these mean values are subtracted from the individual Januarys, Februarys, and so on. The same procedure (step two and three) is applied to the air temperature at the 1000-mb level. Finally, the anomalies are interpolated to the ocean model grid and added to the climatic wind stress of HR and the COADS climatic air temperature, respectively. The reason for using the hybrid dataset is to allow the ocean model to fluctuate around its old equilibrium state, thus saving the computer time that would be necessary to perform a new spinup run (approximately 4000 model years).

To yield wind stress from the ECMWF velocities, a constant drag coefficient of $c_d = 1.2 \times 10^{-3}$ is used, and for the adaption of air temperatures Newtonian coupling is assumed with an adaption rate of $40 \text{ W m}^{-2} \text{ K}^{-1}$. The ocean model is integrated for ten more years with climatological boundary conditions to check for trends in the equilibrium state (mainly for the matter term) and to spin up the wobble equation. After that the model is forced with the transient boundary conditions corresponding to the years 1980 to 1993. The forcing cycle is repeated once, that is, after the first time December 1993 follows the second January 1980 (Fig. 1). Comparison of both periods allow us to distinguish the response to the boundary conditions from trends within the ocean model due to the enhanced variability of the forcing. Results shown are from forcing period two as mainly during the first two years a strong rise in the moment of inertia occurred due to the enhanced variability of the boundary conditions and consequent changes in the convection patterns in high latitudes. Variations in lod are calculated for each month from November 1979 to November 1993 related to an initial

lod of 86 164 seconds, which corresponds to the ocean's state of the climatic January. The contributions of the three aforementioned mechanisms (pressure torque, matter, and motion term) are calculated separately and then summed up. Thereby we assume an instantaneous response of the solid earth's rotation to the pressure torque within the time step of one month. As a closed momentum budget of the solid earth-atmosphere-ocean system is assumed, changes in oceanic angular momentum (due to meridional mass redistributions and variations of zonal currents) must be equalized by corresponding changes in the solid earth's angular momentum.

3. Description of the terms and results

Following Munk and MacDonald (1960), the ocean's behavior on a rotating sphere is described by the Eulerian equations of motion defined in a coordinate system x_i , $i = 1, 2, 3$, that rotates with an angular velocity ω_i relative to a coordinate system fixed in space X_i . Assuming a coincidence of the axis X_i with x_i for the moment considered, this yields

$$M_i = \frac{dH_i}{dt} + \varepsilon_{ijk}\omega_j H_k, \quad (1)$$

where M_i are the components of the torque, H_i the components of angular momentum, and $\varepsilon_{ijk} = 0$, if $i = k$ or $i = j$ or $j = k$, $\varepsilon_{ijk} = +1$, if the indices are in even order (1, 2, 3, . . .), $\varepsilon_{ijk} = -1$, if the indices are in odd order (1, 3, 2, . . .). The total angular momentum H can be decomposed into two parts; that is,

$$H_i = I_{ij}(t)\omega_j + L_i(t) \quad (2)$$

with

$$I_{ij} = \int_V \rho(x_k x_k \delta_{ij} - x_i x_j) dV, \quad (3)$$

where I_{ij} is the tensor of inertia of the mass m of the volume element dV . The mass m is variable in the ocean due to changes in the density of the seawater and due to changes in the surface elevation; δ_{ij} is the Kronecker symbol. The second term on the rhs of (2),

$$L_i = \int_V \rho \varepsilon_{ijk} x_j u_k dV, \quad (4)$$

yields the angular momentum of the motions u_i relative to the main axis of inertia x_i .

By inserting (2) into (1) one yields the Liouville equations

$$M_i = \frac{d}{dt}(I_{ij}\omega_j + L_i) + \varepsilon_{ijk}\omega_j(I_{kl}\omega_l + L_k). \quad (5)$$

These equations describe the three mechanisms of angular momentum exchanges between the ocean and the solid earth: M_i is the torque exerted at the ocean-solid

earth interface, that is, the effect of pressure differences on opposite boundaries of continental margins and submarine topography (henceforth pressure torque); I_{ij} and I_{kl} , respectively, describe the variability caused by changes of the moment of inertia of the ocean, that is, the matter term, and L_i and L_k describe the variability of the oceanic velocity field, that is, the motion term. The single terms will be described in more detail in the following sections. The axis x_3 of the rotating coordinate system is chosen as the main rotation axis of the earth, so that changes in lod (Δlod) are determined by $d\omega_3/dt$, while the components $d\omega_1/dt$ and $d\omega_2/dt$ determine the wobble, that is, the deviation of the main rotation axis of the earth from the celestial pole. The Chandler wobble has been computed, but the interpretation of the data is still in progress and not discussed in this paper.

Figure 2 shows the climatological cycle of matter and motion term. The contributions from sea level and density field are split up to allow comparison with the values of Ponte and Rosen (1994). While there is good agreement for the motion term in phase and amplitude, for the matter term only the phase for the density field term is quite similar while the sea level signal appears to be shifted by 6 months. Additionally, there are discrepancies in amplitude, which is generally larger in our model results. In the following, the single terms will be described. Hereby Δlod means deviation of the computed length of day from the sidereal day, and anomaly of Δlod is the deviation between the computed Δlod for a single month and the Δlod obtained with climatological forcing.

a. Pressure and friction torque

Pressure torques on the continents and submarine topography and hence the solid earth are exerted by the oceans if a zonal pressure gradient across the ocean basin exists. This can be caused either by differences in sea level or the density field. Changes caused by sea level pressure variations are neglected in this study. The zonal pressure torque M_1 is then expressed by

$$M_1 = \sum_{d=1}^N \Delta z(d) \int_{-\pi/2}^{+\pi/2} \int_{-\pi}^{+\pi} \frac{\partial p}{\partial x_1} R^2 \cos x_2 dx_1 dx_2, \quad (6)$$

with

$$p = \rho_0 g \zeta + \int_{-H}^0 \rho g dz,$$

where ρ_0 is the mean density, g acceleration of gravity, $\partial p/\partial x_1$ the zonal pressure gradient ($p_{\text{west}} - p_{\text{east}}$), R the radius of the earth, x_1 the geographical longitude, x_2 the geographical latitude (both dimensionless), and $\sum_{d=1}^N$ the sum over all layers. Here ζ is the sea surface elevation and H the depth of the ocean.

Changes in Δlod caused by the pressure torque are calculated as

SEASONAL CYCLE OF MATTER AND MOTION TERM

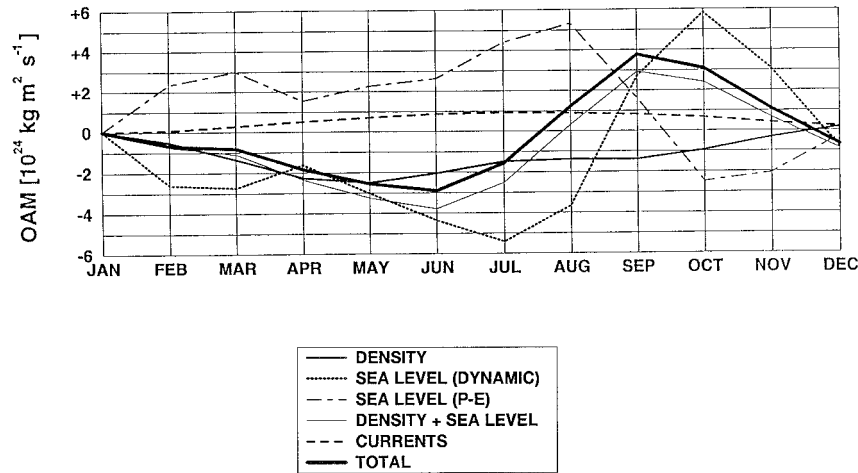


FIG. 2. Seasonal cycle of globally integrated contributions to oceanic angular momentum (OAM) from model results. Shown are the effect of the density field; the effect of the dynamical changes in sea level; the effect of sea level changes due to freshwater fluxes; the combined effect of both sea level contributions and the density field, that is, the matter term; the effect of the zonal velocity field, that is, the motion term; and the combined effect of matter and motion term (refer to legend for meaning of the different line styles). The curves are plotted relative to the climatic January.

$$\Delta \text{lod}(M_1) = \frac{M_1 \cdot \Delta t}{(I_{33}^E + I_{33}) \cdot \Omega_0} \cdot 86\,164 \text{ s}, \quad (7)$$

where I_{33}^E is the moment of inertia of the solid earth relative to its axis of rotation, that is, $8.0205 \times 10^{37} \text{ kg m}^2$; Δt is the model's time step; and Ω_0 is the rotation rate of the earth at $t = 0$, that is $7.29 \times 10^{-5} \text{ s}^{-1}$.

Due to the steady, westward blowing trade winds the sea level is higher at the western boundaries of the equatorial Pacific and Atlantic compared to the eastern boundaries (Wyrki 1985; Peixoto and Oort 1992). The depth of the thermocline, on the other hand, decreases from west to east and the resulting density gradient causes an opposite torque. The meridional distribution of the zonal means of the annual mean pressure torque split up into the sea level and density effect is shown in Fig. 3a. It is seen that the sea level effect slightly dominates. The resulting net torque in low latitudes is directed opposite to the earth's rotation direction in low latitudes. The magnitude of the net torque is by two orders of magnitude smaller than the effect of sea level differences alone, as sea level and density stratification are almost in isostatic balance within the time step of one month.

The zonal friction torque F_1 from the atmosphere to the ocean is calculated as

$$F_1 = \int_{-\pi/2}^{+\pi/2} \int_{-\pi}^{+\pi} R^3 \cos^2 x_2 \tau_1 dx_1 dx_2 \quad (8)$$

with τ_1 the zonal windstress at ocean points. The sign convention here is such that positive friction torque ac-

celerates and positive pressure torque decelerates earth's rotation.

Figure 3b shows that the torque exerted by the wind on the ocean by surface friction is nearly coincident with the inverted torque from ocean to solid earth. This is partly due to the time step of one month used in the model calculations. As former investigations show (Ponte 1990; Ponte and Rosen 1994), the pressure and density fields in the ocean are almost in equilibrium with the atmospheric forcing within two to three weeks. This is because the barotropic modes of the induced waves contain the major part of the energy and are very fast (up to several meters per second). The baroclinic response is by far slower. The curves in Fig. 3b justify the hypothesis of Peixoto and Oort (1992) that the momentum input from the atmosphere to the ocean is transported to the solid earth at constant latitude. In contrast to their values here the friction torque represents only values over the oceans and the pressure torque represents values over the whole depth of the ocean. We confirm the authors' hypothesis that this leads to an almost total coincidence of the curves.

Time series of the pressure torque is shown in Fig. 4 together with the wind friction torque at the ocean surface. The sign convention here is that a westward wind (in opposite direction to the earth's rotation) implies negative friction torque and a positive zonal pressure gradient across the ocean basins (higher sea level at the eastern boundary) implies positive pressure torque.

During the early 1980s, the weakening of the trade

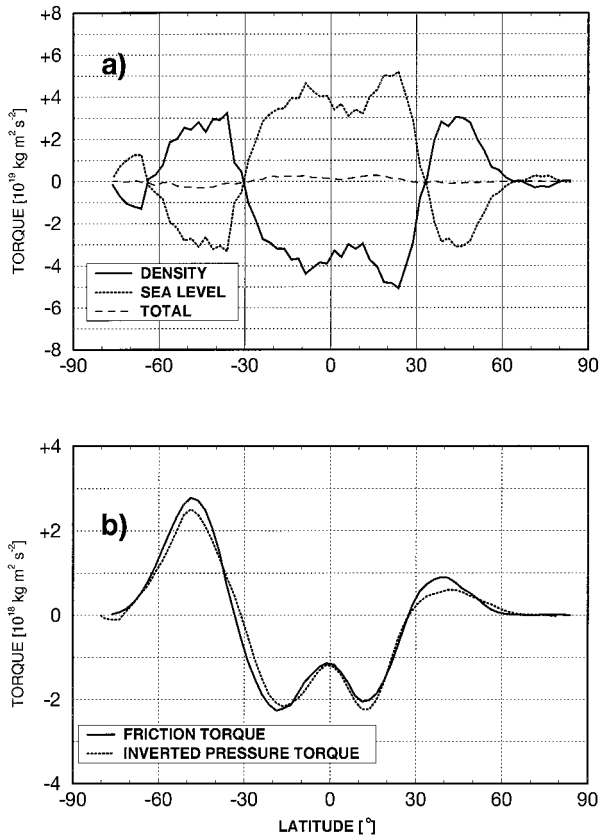


FIG. 3. (a) Zonal means from south to north of the pressure torque due to density (solid) and sea level (dotted) (in kg m² s⁻²) and the combined effect (dashed). (b) Zonal means of wind friction torque input to the ocean (solid) and pressure torque from the ocean to the solid earth (dotted). The dotted curve in (b) is the blown up and inverted dashed curve in (a).

winds during the 1982–83 El Niño results in a reduced zonal sea level gradient across the equatorial Pacific as the piling up of water masses in the western equatorial Pacific is in dynamical balance with the wind forcing. The effect of the decreasing zonal sea level gradient on the pressure torque is only partly compensated by reduced tilting of the thermocline due to the slowness of the baroclinic modes. Hence, the pressure torque in the opposite direction to the earth’s rotation is reduced and thus the earth’s rotation is accelerated. This means that the pure effect of the pressure torque would cause a decrease of the lod during an El Niño.

As for the latitudinal distribution of the annual means (Fig. 3b), variations of the pressure torque in time are transmitted almost completely from the atmosphere to the solid earth by the ocean. The large anomaly in both friction and pressure torque during 1980 is caused by anomalous strong westward winds in high latitudes of the Southern Hemisphere as well as by weak trade winds (not shown here). The values even exceed the 1982–83 friction torque, though no El Niño event occurred in 1980. The ECMWF analyses are, however, not very

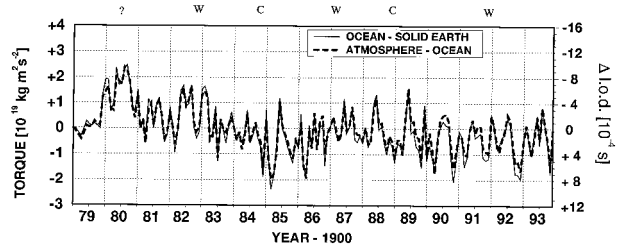


FIG. 4. Time series of global means of friction torque from atmosphere to ocean (dashed) and inverted pressure torque between ocean and solid earth (solid) (in kg m² s⁻²) from 1979 to 1993. The scale for the changes in lod implied by the changes of the respective torques is at the right margin of the figure. El Niño periods are indicated by a W; La Niña periods by a C.

accurate in the early 1980s (Simmons et al. 1995). The Ekman pumping in the Tropics calculated from the ECMWF data shows unrealistic El Niño-like reduced values in 1980 (Fig. 5), so the calculated results for 1980 are doubtful and not discussed any further.

The Δ lod due to the pressure torque are shown in Fig. 4 (axis to the right of the figure). The 1982–83 El Niño signal is clearly seen. Again, the extreme negative values in 1980 seem to be unreliable. For the 1982–83 El Niño the positive anomalies of the friction torque are in agreement with observations as reduced trade winds and reduced zonal sea level and density gradients across the Pacific are observed during warm events (Wyrtki 1985).

At the beginning of 1984 a period with stronger westward winds begins. The corresponding friction torque input to the ocean results in positive lod anomalies with maximum values in early 1985. A sharp rise of friction torque toward positive values takes place during 1985, followed by a second minimum in late 1986. The two events result from changes of the wind field in the ACC region as the signal also appears in the lod changes deduced from the motion term and in the transport rates through Drake Passage (shown later in Fig. 12). The 1986 peak is less pronounced in lod changes due to the pressure torque.

The 1986–87 El Niño is weakly represented in the wind friction torque based on the ECMWF data. However, the trend in the time series of the lod changes (Fig.

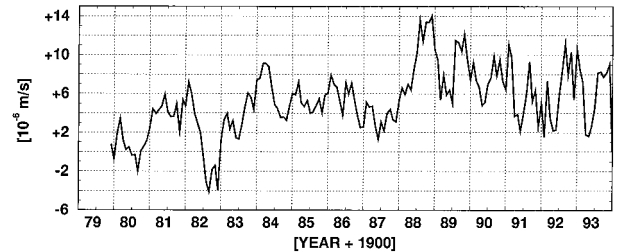


FIG. 5. Time series of the Ekman pumping velocity as derived from the ECMWF wind speed data. Mean over the area extending from 8.75°N to 8.75°S, 150°E to 90°W.

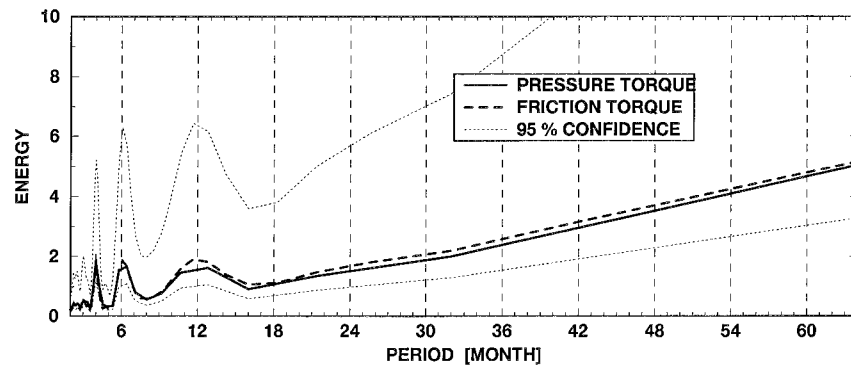


FIG. 6. Power spectrum of the lod change due to pressure torque (solid) and the power spectrum of the normalized wind friction torque input (bold dashed). The thin-dashed line shows the 95% confidence interval of the pressure torque spectrum. The spectral energy is in relative units.

4) is in the same direction as 1982–83 and indicates a slight decrease of lod. The same holds for the weak but long-lasting 1991 event. In general, the changes in lod due to the pressure torque reflect the atmospheric input of zonal momentum in low latitudes, that is, the intensity of the Walker circulation. Single events, however, can be controlled by variations in higher latitudes, mainly in the ACC region where high wind speeds overcome the smaller distance to the rotation axis.

A comparison of the power spectra of the time series of pressure and friction torque (Fig. 6) shows the coincidence of the two spectra. Little energy is found at high frequencies; there are peaks at 3, 6, and 12 months, but the main energy is confined to lower frequencies.

b. Matter term (moment of inertia of the ocean)

The moment of inertia I_{33} relative to the earth's axis of rotation reads

$$I_{33} = \sum_{d=1}^N \int_{-\pi/2}^{+\pi/2} \int_{-\pi}^{+\pi} mR^2 \cos^2 x_2 dx_1 dx_2, \quad (9)$$

where m is the mass of the fluid element depending on temperature, salinity, and pressure at the grid point and for the surface layer, as well on the surface elevation. Changes of the moment of inertia occur if the oceanic mass field is shifted with respect to the rotation axis of the earth. Meridional and vertical redistribution of mass results in variations of the distance between the fluid elements and the rotation axis, thus changing the length of the lever arm. Sea level changes cause net changes of the mass of the water column at a certain latitude. In the ocean, the sea surface elevation and the vertical density stratification tend to balance each other.

Corresponding Δlod values are calculated as

$$\Delta\text{lod}(I_{33}) = (86\,164\text{ s}) \frac{I_{33} - I_{33(t=0)}}{I_{33}^E + I_{33}}. \quad (10)$$

Variations of the density of the water and hence the mass distribution within the ocean occur in response to

variations of the wind-driven and thermohaline circulation. Meridional redistributions of mass have a stronger effect than vertical ones as the vertical extent of the ocean is about one-thousandth of the earth's radius. To estimate the effect, assume that the intertropical convergence zone (ITCZ) is displaced by 10° of latitude. For the zone of upwelling cold water, this causes a change in the distance to the earth's rotation axis of $R(1 - \cos 10^\circ) = 97\text{ km}$. This must be compared to the ocean's upwelling depth of a few hundred meters. As the moment of inertia is proportional to R^2 , the meridional shift results in a change of the moment of inertia of roughly 3%. Stronger or weaker upwelling during El Niño cycles amounts only to changes in the ocean's moment of inertia in the order of 0.1%. Changes of the meridional circulation in the vicinity of the equator are more important than upwelling fluctuations as the poleward advection of water in the surface layer and the equatorward advection in subsurface layers (i.e., the meridional overturning, Fig. 7) determine the subsurface density of the water in the Tropics.

The moment of inertia is also changed by variations of sea level in the tropical Pacific. The water masses that are piled up in the western equatorial Pacific during periods of strong trade winds move to the east during an El Niño and also poleward (Wyrki 1985), that is, to latitudes with a shorter moment arm. This results in a net loss of mass in the equatorial Pacific during an El Niño and hence a reduction of the moment of inertia of the ocean.

Thermal expansion, though not explicit in the model code, can be calculated diagnostically. It modifies the length of the moment arm of a fluid element in the order of centimeters and is therefore negligible.

The change in lod that is related to the matter term is shown in Fig. 8a. The computed seasonal variation of lod is roughly 0.15 ms. The time series of the change of lod related to the matter term (solid) and the motion term (dashed) after elimination of the linear trend and the seasonal cycle are shown in Fig. 8b. A maximum of the matter term is found in late 1980 to early 1981.

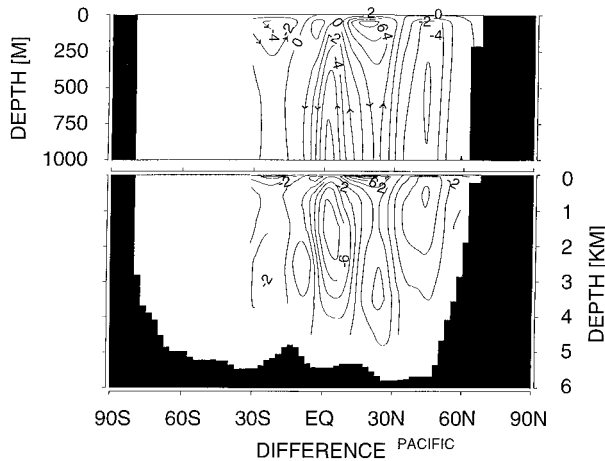


FIG. 7. Difference of the meridional circulation in the Pacific, in Sverdrups, between climatic December and December 1983. The upper 1000 m are blown up in the upper panel. Arrows indicate flow direction. The overturning cell in the North Pacific results from a slight increase in convective adjustment.

Pre-El Niño conditions are characterized by anomalously high sea level in the West Pacific and the build up of a warm water pool. Model results support that with respect to the moment of inertia of the ocean, the sea level rise overcompensates the decrease in density due to the warming of the water. As already mentioned, the results for 1980–81 are uncertain.

A similar but less pronounced signal is predicted for late 1983. With El Niño conditions in the surface layer, one would rather expect a minimum of the matter term at that time due to positive temperature anomalies. We use observations from Tourre and White (1995) to compare them with model results. As the density of the water in the Tropics is mainly controlled by temperature and not by salinity changes we use temperature data for comparison. The calculated temperature averaged over the upper 450 m (which includes values below the thermocline) from 8.75°N to 8.75°S in the Pacific (Fig. 9) clearly shows a negative anomaly at the end of 1983. This is in good agreement with the observations. The lower limit of 450 m was chosen as it represents the depth to which measured data extend in the dataset. The negative temperature anomaly is not only caused by enhanced equatorial upwelling, which shows a maximum in spring 1984 (Fig. 5), but also by a southward shift of the ITCZ (compared to the climatological state) that forces colder north equatorial water toward the equator due to a strengthening of the northern part of the meridional circulation (Fig. 7). From the model, poleward of the equator temperatures at a certain depth are slightly lower in the Northern Hemisphere. As shifts of the ITCZ are connected to changes of the Hadley circulation, this means that the moment of inertia is partly related to the Hadley circulation. This relationship needs further investigation.

The 1988–89 maximum of lod anomalies caused by

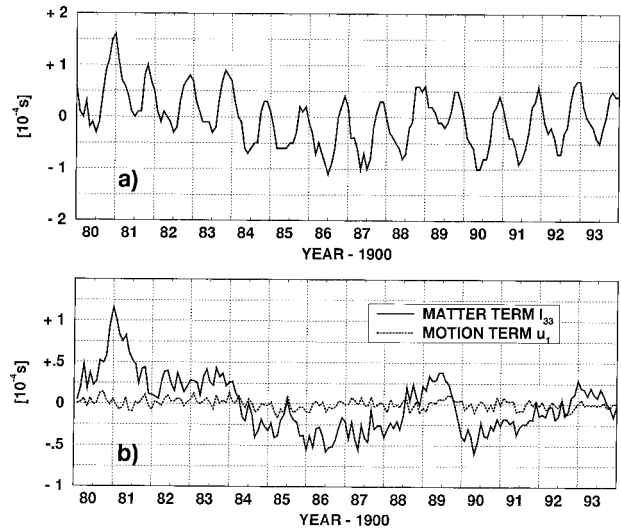


FIG. 8. (a) Time series of the change in lod due to the matter term for the period from 1980 to 1993. The linear trend is removed from the time series. (b) Anomalies of change in lod, that is, deviation from the climatic cycle due to the matter term (solid) and the motion term (dashed).

the matter term is also confirmed by the good agreement of simulated and observed temperatures. The Ekman pumping in the equatorial area (Fig. 5) shows a strong rise at the same time. This leads to a rise of the sea level and a decrease of the temperature, both causing an increase in the moment of inertia (Fig. 8b).

In contrast the 1986–87 El Niño is poorly reproduced in the model (Fig. 9). The calculated temperature anomaly shows negative values, whereas the observed one is even higher than in 1982–83. At the end of 1989 a sharp increase in model temperature occurs resulting in a reduced northern winter maximum and hence negative lod

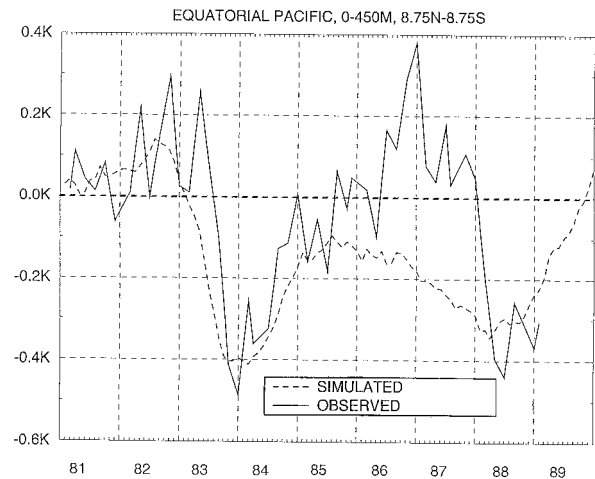


FIG. 9. Time series for the temperature anomaly in the Pacific averaged over a box from 8.75°N to 8.75°S and from the surface down to 450 m. Solid: observations from Tourre and White (1995), dashed: model results. Values are given in kelvin.

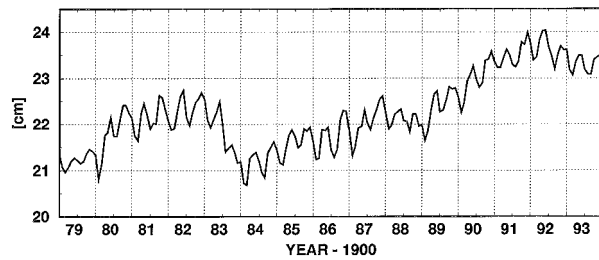


FIG. 10. Time series of the sea level in the equatorial Pacific as derived from model results from 1979 till 1993. Mean value over the area from 8.75°N to 8.75°S, 150°E to 90°W. The total amplitude in the covered period is 3 cm.

anomaly. The calculated sea level in the same area rises also (Fig. 10) but the temperature rise is overcompensating the sea level rise, resulting in a drop of 0.1 ms in lod within 6 months (Fig. 8b). The last four years of the forcing period show a slow rise of lod but without pronounced peaks. The changes of the anomalies of the motion term (described in section 3c) that are shown in Fig. 8b are small compared to the anomalies of the matter term. Also, the interannual variations remain small.

From model results we can conclude that matter term contributions to lod reflect temperature variability more than sea level changes. This is in coincidence with results from Brosche et al. (1990), showing that the effect of density variations on lod are reduced to 10% by the compensating sea level, whereas for absolute values the sea level effect dominates (Fig. 3a). La Niña periods show a stronger signal than El Niño events due to deeper penetration of the anomalies (Fig. 9).

The total amplitude of the lod anomaly referring to the matter term is about 0.15 ms compared to 1.5 ms for those related to the pressure torque. For the comparison of observations and model results it should be kept in mind that changes of the pressure term are contained in the measured data if monthly averaged. This leaves the matter and motion term contributions for filling the gaps.

The spectrum (Fig. 11) of the Δlod time series shows

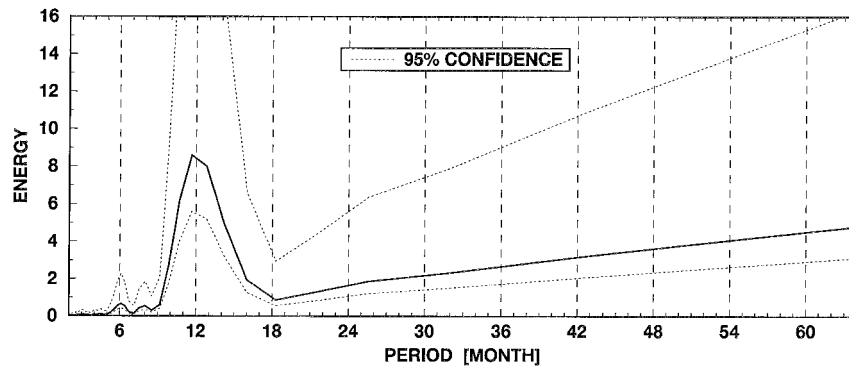


FIG. 11. Power spectrum of lod change due to the matter term. The dotted line shows the 95% confidence interval.

a major peak at annual periods and low energy at high frequencies. More energy is found at periods of several years, reflecting the slow process of mass redistribution. The time series, however, is too short to show a peak at the ENSO frequency of about 5 years.

c. Motion term (angular momentum of ocean currents)

Changes of the motion term are caused by changes in the zonal velocity field and, to a minor extent, by changes in sea level that cause a change of mass of the moving fluid element in the surface layer. Slight violations of the momentum balance with respect to the motion term arise by the use of the Boussinesq approximation and the neglect of the advection of momentum as applied to the LSG. In a strict sense, this means that angular momentum is not exactly conserved in the model. However, given the coarse resolution of the model it can be shown that these violations are negligible except near the equator where the cosine of the latitude varies only slowly.

The angular momentum L_1 stored in the ocean is given by

$$L_1 = \sum_{d=1}^n \int_{-\pi/2}^{+\pi/2} \int_{-\pi}^{+\pi} mu_1 R \cos x_2 dx_1 dx_2, \quad (11)$$

where u_1 is the zonal velocity of the fluid element.

Changes in lod are calculated as

$$\Delta lod(L_1) = (86\ 164\ s) \frac{L_1 - L_{1(t=0)}}{L_1^E + L_1} = 1.46 \times 10^{-29} \Delta L_1, \quad (12)$$

where the superscript E refers to the solid earth. The topic has been studied intensely in the past (e.g., Brosche and Sündermann 1985), presuming that changes in the motion term are mainly controlled by changes in the magnitude of the ACC. In most cases transport values for Drake Passage were estimated and transferred into momentum changes. Certainly the ACC is the major zonal current on the globe. But it is not a priori clear

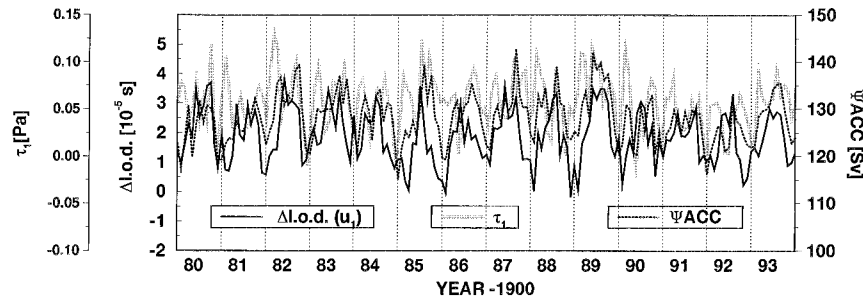


FIG. 12. Time series from 1980 to 1993 for change in lod due to the motion term (solid), simulated transport through Drake Passage (Ψ ACC) in Sverdrups (dotted), and mean wind stress (τ_1) between 50° and 70° S in pascals (solid, gray).

to what extent the other zonal currents, for example, the zonal parts of the Gulf Stream and the Kuroshio and the currents of the equatorial current system balance each other. Peixoto and Oort (1992) assume a total transport of the subtropical gyres of 100 Sv ($\text{Sv} \equiv 10^6 \text{ m}^3 \text{ s}^{-1}$) with westward flow at the equator and eastward flow at 40° latitude. The corresponding momentum difference between westward and eastward flow that is caused by the difference in latitude is $5 \times 10^{24} \text{ kg m}^2 \text{ s}^{-1}$. The contribution of the ACC, assuming a transport of 110 Sv at 50° S, amounts to $1.1 \times 10^{25} \text{ kg m}^2 \text{ s}^{-1}$, and a variation of 20 Sv as it is simulated by the model would imply changes of $2.1 \times 10^{24} \text{ kg m}^2 \text{ s}^{-1}$. Estimates for the variation of the subtropical gyre circulation are rare. From our model output, changes in the order of several tens of Sverdrups, as required for a momentum change comparable to that of the ACC, are confined to latitudes of about 30° , that is, to the center of the gyres. Also, the changes in the Northern and the Southern Hemisphere are of opposite sign and thus balance each other. From this estimation it is deduced that changes in the ACC determine the amplitude of the motion term rather than those of the subtropical gyres. With respect to the currents at the equator, it should be stated that during an El Niño the westward surface current in the equatorial Pacific (the north equatorial countercurrent is not resolved in the model) and the eastward Cromwell

undercurrent in the deeper layers weaken as well, so the net effect is assumed to be small. The time series of the change in lod is shown in Fig. 12 together with transport rates in Drake Passage and the wind stress between 50° and 70° S. There is obviously coincidence between the wind forcing and the transport through Drake Passage. The correlation coefficient $R = 0.577$ between the two time series is significant at the 95% level. We are well aware that our OGCM, as other coarse-resolution circulation models, produces reasonable transport rates in the ACC region only by assuming very high turbulent horizontal viscosities. But after this tuning the transport fluctuation variations in response to the transient wind forcing seem to be in realistic range. It should be mentioned here that presently no global ocean circulation model exists that resolves baroclinic eddies in the ACC region, where the internal Rossby radius is on the order of 5 km.

The annual range of the motion term is large compared to the interannual changes. Total variations amount to about one-fourth of those caused by the matter term compared to one-third for the annual cycle. The corresponding energy spectra are shown in Fig. 13. The transport through Drake Passage and, even more so, the wind stress in the ACC region show a clear semiannual peak, while such a peak is missing in the lod spectrum. This is in agreement with results from Dickey et al.

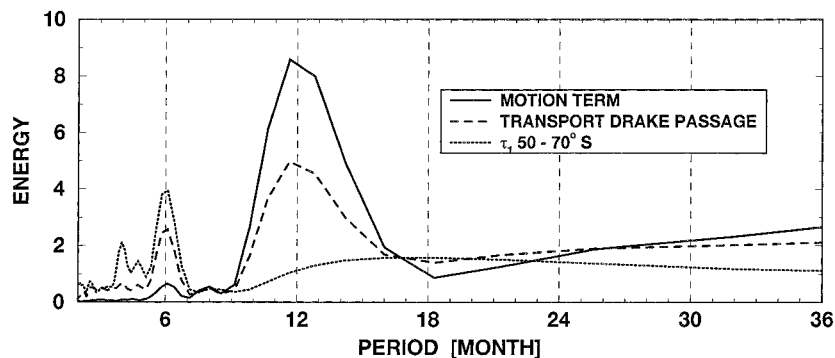


FIG. 13. Power spectra of change in lod due to the motion term (solid), transport through Drake Passage (dashed), and mean wind stress between 50° and 70° S (dotted).

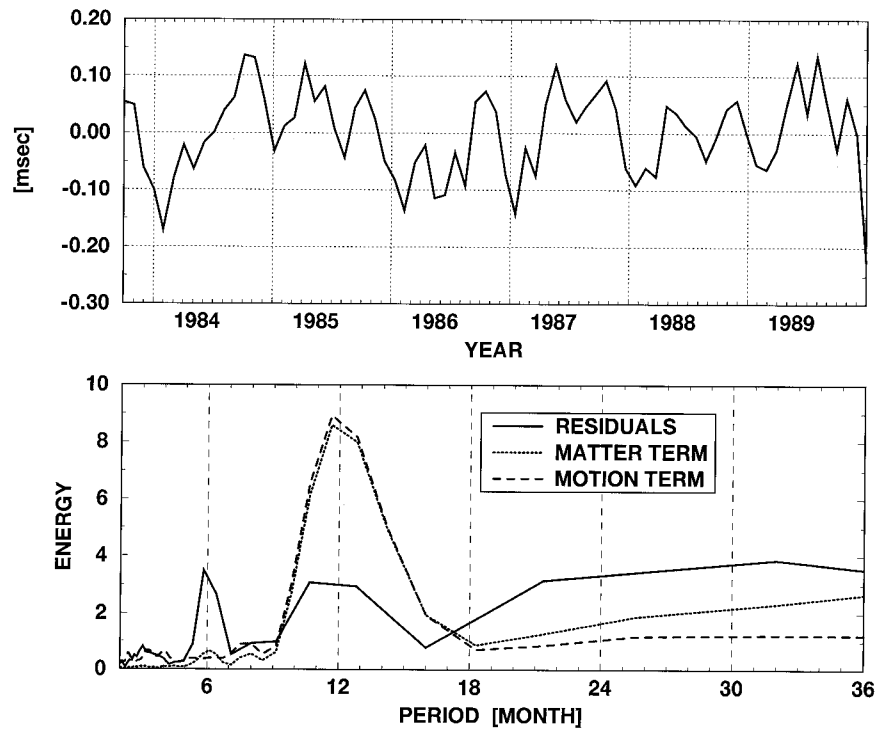


FIG. 14. (a) Residuals of Δ lod (observed minus AGCM 1000 to 100 mb) and anomalies of Δ lod from the matter and motion term. The tides are removed from the residuals. (b) Power spectrum of the residuals (solid), the matter term (dotted), and the motion term (dashed). The energy is in relative units and not comparable, as the time series are normalized by their standard deviation.

(1993), who used results from an experiment with the FRAM model (Webb et al. 1991). The authors argue that the semiannual variations of the ACC are compensated for by currents farther to the north.

d. Residuals

Residuals of observed data and AGCM calculations of lod are shown in Fig. 14a together with the anomalies of matter and motion term. The figure shows the observed *Delta* lod minus the Δ lod computed with an AGCM. The model's atmosphere extends from 1000 to 100 mb and the tidal terms as well as a polynomial of third degree are subtracted from the curve (data kindly provided by J. Wunsch based on data from the International Earth Rotation Service in Paris). The data cover a period extending from October 1983 to December 1989. There is no clear coincidence with anomalies of the matter nor the motion term as seen by eye. The correlation between residuals and anomalies of the matter term is only weak ($R = 0.156$) and not significantly different from zero at the 95% level ($z_\alpha = 0.26$). The order of magnitude of the residual Δ lod, however, is about 0.2 ms as in the model results of the matter term. Comparing the anomalies of the residuals (seasonal cycle subtracted) with the anomalies of the matter term leads to a slightly higher correlation ($R = 0.207$).

In Fig. 14b, the spectrum of the residuals is presented.

The spectrum shows peaks at 6 and 12 months. A part of the semiannual variations is thought to be caused by the stratosphere, which is not included in the AGCM used to determine the residuals. The peak at 12 months is in agreement with the respective peaks of the spectra of the matter term (Fig. 14b, dotted) and the motion term (Fig. 14b, dashed) as is the general shape of the spectra besides from the semiannual peak. Thus, support is given that the matter term and motion term can explain at least a part of the residual change in lod. Longer time series of observed residuals and improved boundary conditions for the ocean model, like ECMWF reanalysis, may give further insight in the ocean's role in the angular momentum budget.

4. Conclusions

Results show the expected transport of wind friction momentum input via pressure torque to the solid earth. This almost total transfer takes place zonally and instantaneously in time within the model time step of one month. It turns out that the mass redistribution (matter term) causes around four times more variability than the direct angular momentum (motion term), and that these variations in Δ lod are in the order of 0.1 ms, that is, in the order of observed discrepancies. A comparison of the model results with observed residuals shows no clear coincidence. The spectra of the residuals, the matter

term, and the motion term however are quite similar. The matter term shows most of its variability at annual to interannual timescales, whereas the motion term varies mainly annual.

Considering the basic mechanisms of angular momentum flux we state that changes in pressure torque are to first order caused by changes in the Walker circulation (i.e., intensity of the trade winds), changes of the matter term by changes of the Hadley circulation (i.e., the meridional wind field in the equatorial Pacific) and changes of the motion term are determined by variations of the zonal winds in the ACC region. Remaining problems that are not solved are the role of the freshwater fluxes that are only of climatological nature in the present model calculations, transport of momentum by eddies, and probably the poor resolution of equatorial Kelvin waves and, hence, the delayed action oscillator that in turn is important for a proper description and modeling of ENSO cycles.

Acknowledgments. We thank Ernst Maier-Reimer and P. Brosche for helpful comments and discussions and the “Deutscher Wetterdienst” for providing the ECMWF data. We also wish to thank J. Wunsch for the submission of the residuals of lod and two anonymous reviewers for their efforts in improving the manuscript.

REFERENCES

- Brosche, P., and J. Sündermann, 1985: The Antarctic circumpolar current and its influence on the earth's rotation. *Dtsch. Hydrogr. Z.*, **38**, 1–6.
- , J. Wunsch, A. Frische, J. Sündermann, E. Maier-Reimer, and U. Mikolajewicz, 1990: The seasonal variation of the angular momentum of the oceans. *Naturwissenschaften*, **77**, 185–186.
- Dickey, J. O., S. L. Marens, C. M. Johns, R. Hide, and S. P. Thompson, 1993: The oceanic contribution to the earth seasonal angular momentum budget. *Geophys. Res. Lett.*, **20**(24), 2953–2956.
- Hellerman, S., and M. Rosenstein, 1983: Normal monthly wind stress over the World Ocean with error estimates. *J. Phys. Oceanogr.*, **13**, 1093–1104.
- Lambeck, K., 1980: *The Earth's Variable Rotation. Cambridge Monographs on Mechanics and Applied Mathematics*, 449 pp.
- Levitus, S., 1982: *Climatological Atlas of the World Ocean*. NOAA Prof. Paper No. 13, U.S. Govt. Printing Office, 173 pp.
- Maier-Reimer, E., U. Mikolajewicz, and K. Hasselmann, 1993: Mean circulation of the Hamburg OGCM and its sensitivity to the thermohaline forcing. *J. Phys. Oceanogr.*, **23**, 731–757.
- Munk, W. H., and G. J. F. MacDonald, 1960: *The Rotation of the Earth. Cambridge Monographs on Mechanics and Applied Mathematics*, Cambridge University Press, 323 pp.
- Peixoto, J. P., and A. H. Oort, 1992: *Physics of Climate*. Amer. Inst. Phys., 520 pp.
- Ponte, R. M., 1990: Barotropic motions and the exchange of angular momentum between the oceans and solid earth. *J. Geophys. Res.*, **95**(C7), 11 369–11 374.
- , and R. D. Rosen, 1994: Oceanic angular momentum and torques in a general circulation model. *J. Phys. Oceanogr.*, **24**, 1966–1977.
- Rosen, R. D., and A. Salstein, 1986: Earth rotation as a proxy for interannual variability in atmospheric circulation, 1860–present. *J. Climate Appl. Meteor.*, **25**, 1870–1877.
- , —, T. M. Eubanks, J. O. Dickey, and J. A. Steppe, 1984: An El Niño signal in atmospheric angular momentum and earth rotation. *Science*, **225**, 411–414.
- Salstein, D. A., and R. D. Rosen, 1984: El Niño and the earth's rotation. *Oceanus*, **27**(2), 52–57.
- Segschneider, J., 1991: Windinduzierte Variabilität in der Warmwassersphäre von 1981–1987. Teil I, Datenaufbereitung und SST, Diplomarbeit im Fach Ozeanograph., University of Hamburg, Germany, 101 pp.
- Simmons, A. J., R. Mureau, and T. Petroligias, 1995: Error growth and estimates of predictability from the ECMWF forecasting system. *Quart. J. Roy. Meteor. Soc.*, **121**, 1739–1771.
- Tourre, Y. M., and W. B. White, 1995: ENSO signals in global upper ocean temperature. *J. Phys. Oceanogr.*, **25**, 1317–1332.
- Webb, D. J., P. D. Killworth, D. Beckles, B. A. De Cuevas, R. Offiler, and M. Roe (FRAM Group), 1991: An eddy-resolving model of the Southern Ocean. *Trans. Amer. Geophys. Union*, **72**, 169–175.
- Winguth, A. M. E., M. Heimann, K. D. Kurz, E. Maier-Reimer, U. Mikolajewicz, and J. Segschneider, 1994: El Niño–Southern Oscillation related fluctuations of the marine carbon cycle. *Global Biogeochem. Cyc.*, **8**(1), 39–63.
- Woodruff, S. D., R. J. Slutz, R. L. Jenne, and P. M. Steurer, 1987: A Comprehensive Ocean–Atmosphere Data Set. *Bull. Amer. Meteor. Soc.*, **68**, 1239–1250.
- Wyrtki, K., 1985: Water displacements in the Pacific and the genesis of El Niño cycles. *J. Geophys. Res.*, **90**, 7129–7132.
- Zheng, D. W., G. X. Song, and S. F. Luo, 1990: El Niño prediction. *Nature*, **348**, 119.